scientific reports

Check for updates

OPEN

A multi-scale pipeline linking drug transcriptomics with pharmacokinetics predicts in vivo interactions of tuberculosis drugs

Joseph M. Cicchese[1], Awanti Sambarey[2], Denise Kirschner[3]✉, Jennifer J. Linderman[1]✉ & Sriram Chandrasekaran[2]✉

Tuberculosis (TB) is the deadliest infectious disease worldwide. The design of new treatments for TB is hindered by the large number of candidate drugs, drug combinations, dosing choices, and complex pharmaco-kinetics/dynamics (PK/PD). Here we study the interplay of these factors in designing combination therapies by linking a machine-learning model, INDIGO-MTB, which predicts in vitro drug interactions using drug transcriptomics, with a multi-scale model of drug PK/PD and pathogen-immune interactions called *GranSim*. We calculate an in vivo drug interaction score (iDIS) from dynamics of drug diffusion, spatial distribution, and activity within lesions against various pathogen sub-populations. The iDIS of drug regimens evaluated against non-replicating bacteria significantly correlates with efficacy metrics from clinical trials. Our approach identifies mechanisms that can amplify synergistic or mitigate antagonistic drug interactions in vivo by modulating the relative distribution of drugs. Our mechanistic framework enables efficient evaluation of in vivo drug interactions and optimization of combination therapies.

Tuberculosis (TB), caused by inhalation of *Mycobacterium tuberculosis* (Mtb), remains the world's deadliest infectious disease, infecting 30% of all people world-wide and leading to ~ 1.3 million deaths annually[1,2]. The emergence of multidrug resistance coupled with slow progress in developing new drugs has created a pressing need to identify new approaches to treat TB. The current standard TB treatment regimen is a combination of four first-line anti-TB drugs—the antibiotics isoniazid (H), rifampicin (R), pyrazinamide (Z), and ethambutol (E). This treatment has remained unchanged over 50 years[3–5]. Typical combination therapy for TB is administered for at least six months, while treating drug-resistant strains may take up to 2 years. New drugs, such as bedaquiline, linezolid, and pretomanid, are being tested in new regimens to potentially shorten TB treatment[6,7] The WHO has called for entirely new strategies to meet the goals for 'End TB', which aims to reduce TB deaths by 95% by 2035.

The large number of potential drug combinations greatly complicates TB treatment design[8]. Therapy involving drug combinations can lead to surprising non-linear effects; some drugs can enhance each other's action leading to higher potency (synergy), or drugs can interfere with their action leading to reduced potency (antagonism)[9,10]. Antibiotics can interact synergistically by enhancing the uptake of other drugs or through inhibition of compensatory mechanisms. For example, ethambutol represses the levels of the enzyme *inhA,* the drug-target of isoniazid and enhances the bactericidal effect of isoniazid against Mtb[11]. Similarly, antagonistic interactions between bacteriostatic drugs and bactericidal drugs occur due to their opposing effects on cellular metabolism[12]. Drug interactions can impact treatment efficacy and emergence of drug resistance[13]. Synergistic drug combinations can also provide increased efficacy without augmenting the toxicity of individual drugs.

Such synergistic or antagonistic drug interactions can be determined using checkerboard assays by screening a panel of drug combinations in multiple doses against Mtb[14]. However, such experimental screening of drug interactions has limited throughput despite recent developments in reducing the number of doses required for

[1]Department of Chemical Engineering, University of Michigan, Ann Arbor, MI, USA. [2]Department of Biomedical Engineering, University of Michigan, Ann Arbor, MI, USA. [3]Department of Microbiology and Immunology, University of Michigan Medical School, Ann Arbor, MI, USA. ✉email: kirschne@umich.edu; linderma@umich.edu; csriram@umich.edu

measurement[15–17]. Designing an optimal 4-drug combination from a set of just 50 candidate drugs at a single dose requires ~200,000 drug interaction experiments. The dosage and dosing frequency further increase the space of possible regimens exponentially[18].

Measuring in vivo drug interactions is even more challenging as it requires mice, primates, or other model organisms infected with Mtb[19]. Consequently, the number of drug candidates that can be screened through these model organisms is very limited. Further, current drug screening strategies for TB do not consider a patient's immune system. Once Mtb is inhaled, it triggers a cascade of immune responses that result in the accumulation of an immune cell-rich mass around infected cells and bacteria known as a granuloma. Mtb can persist for decades within granulomas, and there are multiple granulomas within lungs of infected patients[20]. Granulomas also create a physical barrier altering the penetration of drugs, which can greatly impact relative drug concentrations at the site of infection and lead to effective mono-therapies in granulomas[21–24]. Granulomas also produce nutrient-starved and hypoxic environments that contain Mtb that are phenotypically tolerant to antibiotics, further complicating treatment[25,26].

This study addresses these challenges by creating a multi-scale pipeline combining two cutting-edge computational approaches, operating at different biological scales, to evaluate combination therapies using drug transcriptomics and pharmacokinetics/pharmacodynamics (PK/PD) (Fig. 1). First, to rapidly predict drug–drug interactions (synergy/antagonism) among combinations of two or more drugs, we utilize the existing in silico tool—inferring drug interactions using chemogenomics and orthology (INDIGO) optimized for Mtb (INDIGO-MTB)[8,14]. INDIGO-MTB uses a training data of known drug interactions along with drug transcriptomics data as inputs. INDIGO-MTB then utilizes a machine-learning algorithm to identify gene expression patterns that are predictive of specific drug–drug interactions. Once trained, INDIGO-MTB can determine if new drugs in combination have synergistic or antagonistic interactions using transcriptomics data. We previously used INDIGO-MTB to identify synergistic drug regimens for treating TB from over a million possible drug combinations using the pathogen response transcriptome elicited by individual drugs. The INDIGO-MTB model contains 164 drugs with anti-TB activity and it accurately predicted novel interactions of two-drug and three-drug combinations in vitro[8].

Next, to predict in vivo interactions and efficacy, here we integrate INDIGO-MTB predicted drug interactions within an existing multi-scale model of pathogen-immune dynamics leading to granuloma formation, known as *GranSim*[24,28–31]. *GranSim* integrates spatio-temporal host immunity, pathogen growth and drug PK/PD into a single computational framework. *GranSim* uses a hybrid agent-based model to describe interactions between immune cells and cytokines with bacteria and antibiotic delivery to granulomas, and provides a dynamic picture of pathogen clearance leading to granuloma sterilization[24]. Previously, we modeled PK/PD in *GranSim* and explored regimens with isoniazid and rifampin, three fluoroquinolones, and more recently HRZE[32–34]. An important finding from that work is that the various antibiotics have different abilities to penetrate well into the granuloma, at times reducing the number of bacteria exposed to effective concentrations[34,35]. However, in these studies we assumed no interaction between antibiotics. Hence, we now integrate INDIGO-MTB predictions of drug interactions within the *GranSim* framework, allowing the full characterization of drug interaction dynamics at the molecular and cellular scales, and verify our results against patient-level data. This allows us to evaluate how drug interactions and PK/PD at the molecular scale influence in vivo efficacy at the granuloma scale.

Our study herein represents the first pipeline that incorporates both in vitro drug interactions and in vivo PK/PD to simulate treatment dynamics of numerous drug regimens. Our study overcomes the limitation of prior studies that have focused on variation in PK/PD parameters alone to predict treatment outcome[36–38]. Combining INDIGO-MTB with *GranSim* allows us to compare different regimens based on the impact of their interactions on various simulated metrics such as rate of pathogen load decline in granulomas and granuloma sterilization rates. Our approach provides a measurement of drug interactions within lung granulomas based on concentrations that different bacterial populations are experiencing in their individual granuloma environment.

Results

Drug interactions significantly impact in vivo treatment dynamics in GranSim. We focus on combinations of 2, 3 or 4 drugs involving the first-line antibiotics and two fluoroquinolones (Supplementary Table 1). These drugs include isoniazid (H), rifampin (R), ethambutol (E), pyrazinamide (Z), moxifloxacin (M), and levofloxacin (L). We chose these drugs as they are part of the current standard-of-care for treating TB. Further, transcriptomics and PK/PD parameters are available for these drugs for simulation using both INDIGO-MTB and *GranSim*.

Using INDIGO-MTB, we first predicted all possible in vitro interaction outcomes for these combinations. The combinations are predicted to have FIC values that range from synergistic (e.g. HRZ—FIC of 0.74) to antagonistic (e.g. RM—FIC of 2.31). The standard regimen (HRZE) is predicted to be synergistic (FIC—0.82) while moxifloxacin-containing regimens were mostly antagonistic (Supplementary Table 2). These predictions match the experimentally observed in vitro FIC values for these combinations from prior studies[8].

Given the various factors that can impact antibiotic efficacy in vivo that are captured in *GranSim*, the relative impact of drug interactions on treatment outcomes is unclear. We hypothesized that analysis of various drug regimens with different drug interaction scores (FIC) can help tease out the impact on treatment outcome. Our previous studies of antibiotic treatment using *GranSim* did not consider drug interactions. Here we explore how either antagonistic or synergistic affects overall efficacy using *GranSim*.

We input FIC values into *GranSim* and simulated the immune response and antibiotic delivery to granulomas ("Methods"). The plasma and tissue PK parameters for these drugs within the *GranSim* computational framework were derived from previous studies calibrating PK parameters to experimental plasma and lesion drug concentrations ("Methods"). For each regimen tested, 100 simulated granulomas were treated for up to

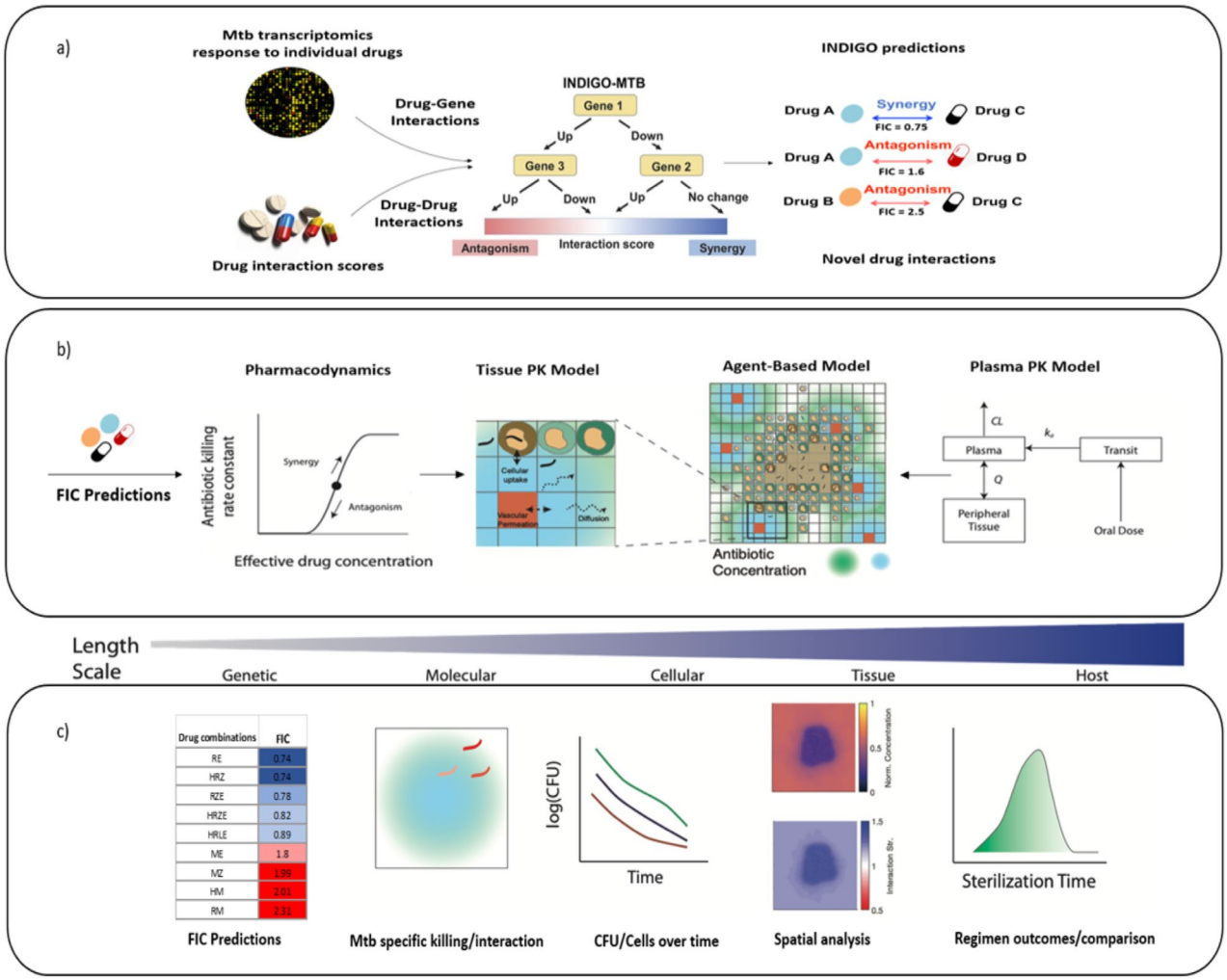

Figure 1. Overview of our multiscale pipeline to predict in vivo drug interactions. (**a**) INDIGO-MTB uses Mtb transcriptomic responses to drugs and experimentally measured drug–drug interactions as inputs for training a machine-learning model, inferring synergistic and antagonistic interactions between new drug combinations as output[8,27]. (**b**) Components of the model integrating *GranSim* and INDIGO-MTB. From right to left, the plasma PK model determines the time-dependent concentration of all antibiotics following oral doses, which in turn determines the amount of antibiotic delivered onto the agent-based model grid. The computational grid is 200 × 200 square grid spaces, representing 4 mm × 4 mm of lung. Within the agent-based model, the tissue PK model describes antibiotic diffusion and binding as well as immune cell accumulation. Based on the local concentration of antibiotics, the PD model evaluates an antibiotic killing rate constant based on an effective concentration that is calculated from each individual antibiotic concentration. The corresponding FIC predicted from INDIGO-MTB either increases or decreases this effective concentration, depending on whether the combination is synergistic or antagonistic. (**c**) Different predictions and outcomes, with the gradient above corresponding to the relevant length scale for the model/prediction. From left to right, predictions made by integration of *GranSim* and INDIGO-MTB are shown, including FIC predictions from INDIGO-MTB, Mtb-specific killing rate and interactions, number of cells/Mtb overtime used to evaluate simulated EBA, spatial analysis of antibiotic concentration and interactions, and sterilization time distributions from a collection of granulomas.

180 days with daily doses of each antibiotic in the specified regimen. To compare the efficacy of each of these regimens, we evaluate three measures: the log decrease in CFU per day, percent sterilization of granulomas, and average sterilization time.

The in vitro FIC value of each combination is correlated with each of the three simulated efficacy outcomes that we calculated (Fig. 2). For our simulated log decrease in CFU per day from 0 to 14 days and the sterilization percent, we observe that both outcomes tend to decrease as FIC values go from synergistic to antagonistic (correlation $R = -0.52$ and -0.59, respectively, Fig. 2A,B). The average sterilization time is positively correlated with FIC value (correlation $R = 0.59$, Fig. 2C). Overall, this indicates that synergistic regimens are more likely to sterilize a greater percentage of granulomas in a shorter time at both early and later time points.

Although these relationships show moderate levels of correlation, there are a few notable deviations. Interestingly, the regimen RM (FIC = 2.31) performs better than the less antagonistic regimen HE (FIC = 1.46). The

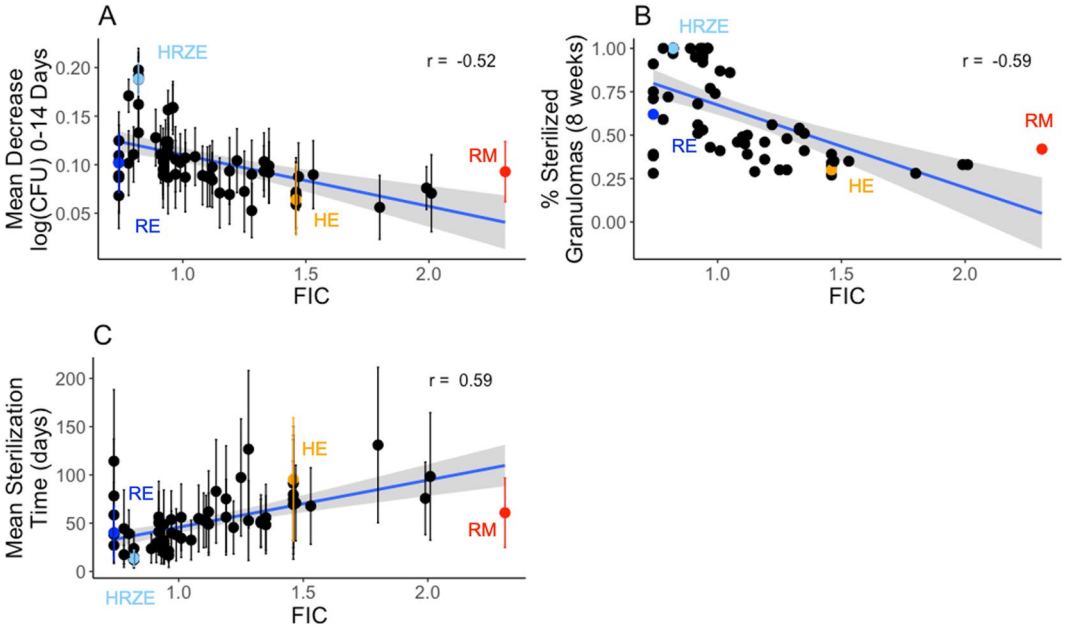

Figure 2. Regimen efficacy is correlated with FIC for 64 simulated drug regimens. Mean decrease in log CFU (0–14 days) averaged over 100 granulomas simulated for each drug regimen (**A**) and percentage of sterilized (negative) granulomas after 8 weeks of treatment (**B**) are negatively correlated with FIC values, with correlation coefficients of −0.52 and −0.59, respectively. Mean sterilization time for each regimen over 100 granulomas (**C**) is positively correlated with FIC with a correlation coefficient of 0.59. Each point represents the regimen outcome measurement for a given regimen and error bars indicate ± standard deviation from the sample of 100 granulomas simulated. The 64 drug regimens simulated are listed in Supplementary Table 1. The colored points correspond to the regimens HRZE (light blue), RE (dark blue), RM (red) and HE (orange) for emphasis. Plots were made using the ggplot2 package in R[39].

best regimen in terms of average sterilization time is HRZE (FIC = 0.82); however, the regimen RE (FIC = 0.74) has a lower FIC but does not perform as well as HRZE. These results suggest that FIC values are not the only factor impacting granuloma sterilization. Because these results are based on sterilization in granulomas, the concentrations of each antibiotic in the granuloma compartment (based on dosage and PK) also impact the ability of each regimen to sterilize.

The in vivo drug interaction score is predictive of treatment dynamics. The antibiotic killing rate is dependent not only on the FIC value, but also on local drug concentrations within a granuloma, the subpopulation of bacteria (intracellular, extracellular replicating, extracellular non-replicating), and the specific PD parameters of antibiotics involved. Based on the definition of the FIC, synergistic or antagonistic drug combinations result in a lower or higher effective concentration to achieve the same level of bacterial killing. To evaluate the overall impact of drug interactions on the calculated killing rate constant, we evaluate an in vivo *Drug Interaction Score* (iDIS) for the three subpopulations of bacteria. The iDIS measures the relative increase or decrease of the antibiotic killing rate constant due to the specific drug interaction. We calculate iDIS as the ratio of the antibiotic killing rate constant evaluated in the simulation to the rate constant if the interaction is simply additive (FIC equal to 1.0). This ratio provides a measure of how much the drug interaction impacts the killing rate constant and is unique for each individual mycobacterium within *GranSim* as drug concentrations change over time. At each time step during treatment, the average iDIS over all Mtb by subpopulation is evaluated as a model output.

Figure 3 shows the average iDIS for non-replicating Mtb over the first dose interval for each regimen, and its relationship to regimen outcomes. A value of 1 indicates the interaction has no impact on the killing rate constant; values greater than 1 or less than 1 indicate synergistic or antagonistic combinations, respectively.

The iDIS for each regimen is strongly correlated with the outcomes from our *GranSim* simulations: log decrease in CFU per day (R = 0.86), percentage of negative granulomas at eight weeks (R = 0.73), and the average sterilization time (R = −0.73) (Fig. 3). The correlations are much stronger than those observed for FIC (Fig. 2), indicating that measuring the iDIS, which is calculated for specific granuloma environments, provides more information on regimen efficacy than examining FIC values, which are calculated based on in vitro environments.

Each combination of antibiotics has a different absolute killing rate constant based on the specific combination of PD parameters associated with that combination together with the distribution of antibiotics within a granuloma. These results suggest that iDIS provides a more accurate representation of how well a given combination of antibiotics achieves sterilization as it accounts for the unique killing rate constant that each individual Mtb experiences and measures the impact that an FIC value has on that killing rate constant.

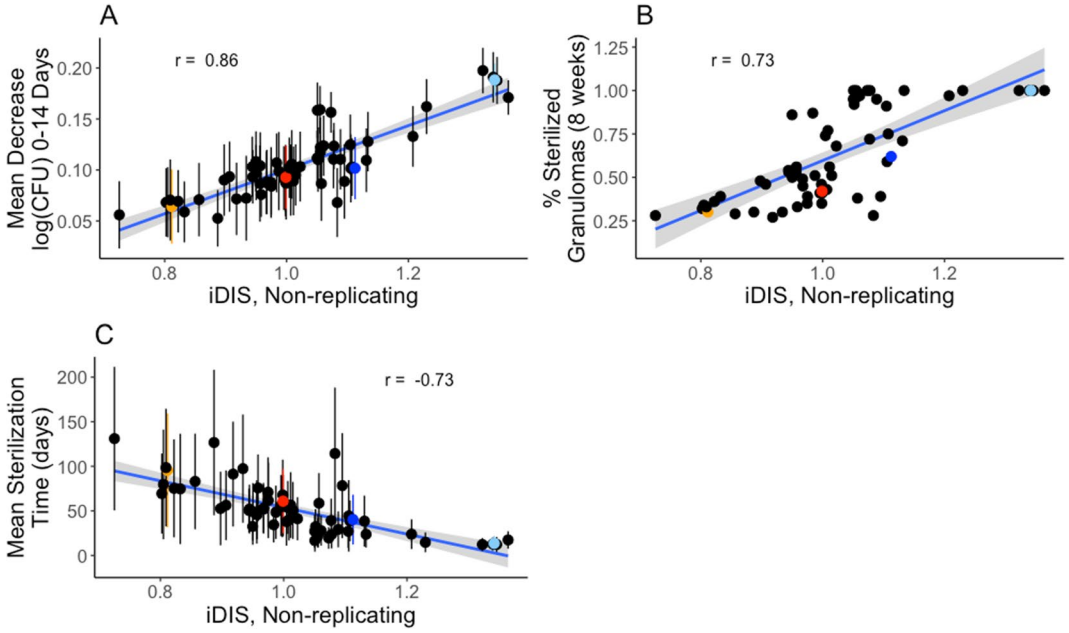

Figure 3. Regimen efficacy is correlated with the in vivo Drug Interaction Score (iDIS). iDIS associated with non-replicating Mtb killing is evaluated for 3 measures over 64 simulated drug combination regimens. The decrease in log CFU (0–14) averaged over 100 granulomas simulated for each regimen (**A**) and percentage of sterilized (negative) granulomas after eight weeks of treatment (**B**) are positively correlated with iDIS of non-replicating Mtb during the first 24 h of treatment (correlation coefficients of 0.86 and 0.73, respectively). Mean sterilization time for each regimen over 100 granulomas (**C**) is negatively correlated with iDIS of non-replicating Mtb (correlation coefficient of − 0.73). Each point represents the regimen outcome measurement for a given regimen and error bars indicate ± standard deviation from the sample of 100 granulomas simulated. The 64 drug regimens simulated are listed in Supplementary Table 1. The colored points correspond to the regimens HRZE (light blue), RE (dark blue), RM (red) and HE (orange) for emphasis. Plots were made using the ggplot2 package in R[39].

Antibiotics are typically better at killing replicating Mtb than non-replicating Mtb. Antibiotic killing rate constants that are higher and closer to their overall E_{max} value are less impacted by drug interactions. We found that correlations between regimen outcomes and the average iDIS associated with replicating extracellular and intracellular Mtb are weaker than when comparing regimen outcomes to the iDIS from non-replicating Mtb (Supplementary Figs. 1 and 2). The average iDIS measurements for replicating Mtb are closer to 1.0 and weaken the correlation with regimen outcomes. Hence, the strong correlation between drug interactions and clinical outcomes are primarily driven by drug action against non-replicating bacteria.

Figure 4 shows a heat map of the mean sterilization time, iDIS and FIC for each regimen, ordered by decreasing iDIS. In general, the regimens with the fastest sterilization times also have high iDIS. The top 17 regimens, as measured by shortest average sterilization time, all contain RIF, indicating that RIF is a very important addition to regimens. Another general trend is that two-drug combinations typically perform worse than 3- or 4-drug combinations. Fluoroquinolones tend to participate in more antagonistic combinations, as measured by the iDIS. For example, 22 of the 31 MXF or LVX containing regimens are above the median iDIS of all 64 regimens. Two regimens (R23.5E45dpw2 and R23.5E90dpw1) with synergistic iDIS measurements showed slow sterilization times, as they were dosed less frequently than a day.

INDIGO-MTB—*GranSim* regimen rankings are correlated with clinical rankings. To explore how our predictions of regimen efficacy compare to clinical results, we compare our INDIGO-MTB—*GranSim* treatment simulations to results from TB drug clinical trials. Drawing from the meta-analysis of phase II trials presented in Bonnet et al., we selected all regimens that reported sputum culture conversion in solid media[40]. The efficacy metric presented for Phase IIb trials is the percent of patients with negative sputum culture after 8 weeks of therapy. Since our simulations predict treatment outcomes at the granuloma scale, we estimated how sterilization at the granuloma level relates to host-level culture conversion. Figure 5A shows the comparison of the upper and lower bound estimates for percent sputum conversion from our simulation to clinical trial results for 26 regimens ("Methods"). For most regimens, estimates of sterilization percentage compare closely to clinically measured culture conversion. In general, *INDIGO-MTB—GranSim* simulations appear to overpredict the rates of sterilization and most incorrect predictions fall into this category (Fig. 5A). This observed overprediction is likely due to the simplification of predicting sterilization at the granuloma scale that does not include the full spectrum of complex granuloma lesions, failed adherence to regimens, and other factors that complicate TB treatment.

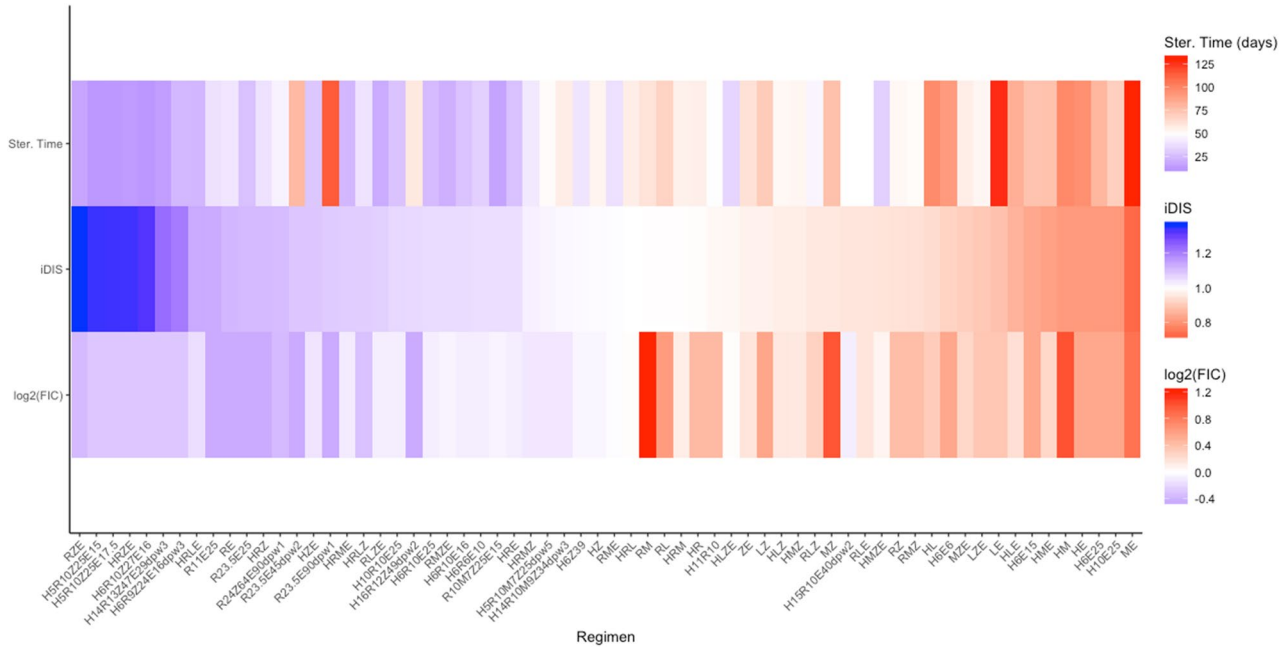

Figure 4. Heat map capturing three metrics for 64 different regimens. The list of regimens is ordered by decreasing predicted iDIS (middle row). For each regimen, the $\log_2$(FIC) value (bottom row) and the average predicted granuloma sterilization time (top row) are also represented. For predicted iDIS and FIC, blue represents synergy, white represents additivity, and red represents antagonism. For sterilization time, blue represents shorter sterilization times and red represents longer. Heat maps were made using the ggplot2 package in R[39].

We next validate our simulation results by comparing the ranking of the efficacy of each of the regimens with the corresponding ranking of the efficacy from clinical trials (Fig. 6). The clinical rank is determined by ranking each regimen by the pooled culture conversion after 8 weeks, so that a ranking of 1 is the regimen with the lowest culture conversion. The simulation rank is determined by percentage of granulomas sterilized after 8 weeks. We used the Spearman ranked correlation coefficient, weighted by the number of patients in each pooled regimen result, and found a significantly strong correlation between simulations and clinical trials ($R = 0.72$).

Recent phase III clinical trials have investigated the impact of introducing fluoroquinolones into treatment regimens to treat drug-susceptible TB, some with the additional intent of shortening treatment time from six months to four. Many of these trials have failed to show improvement in TB treatment, and often led to higher rates of unfavorable outcomes at the trial's endpoints[41–43]. These trends are reflected in our analysis of the drug interactions for various drug combinations. The control regimen, HRZE, is strongly synergistic as measured by iDIS, and we predict short average sterilization times (14 days, Fig. 4). In contrast, fluoroquinolone containing regimens, such as HRMZ and RMZE, are closer to additive, and are predicted to have longer sterilization times of 41 and 21 days, respectively. These trends indicate that our simulation predictions are consistent with phase III clinical trial observations. Thus INDIGO-MTB—*GranSim* simulations provide strong predictive measures of clinical outcome for different regimens.

Both iDIS and INDIGO-MTB FIC predictions for these regimens are also significantly correlated with their clinical ranking (Fig. 5B,C). These simulated results are consistent with the correlation observed in a prior study between INDIGO-MTB FIC scores and percentage of patients with negative culture after treatment from 57 randomized clinical trials[8]. Based on these results, both interaction measurements have the potential to help predict the clinical efficacy of drug combination regimens.

The FIC value is one measure of drug interactions in vitro; however, there are many factors that impact regimen efficacy in vivo that FIC alone does not capture. Measuring the iDIS can incorporate changes in concentration due to PK variability, changes to dosing regimens, and heterogeneous antibiotic concentrations due to granuloma structure and the varying environments where bacteria reside. It also includes effects of the immune responses occurring with granulomas.

Spatial variation in drug concentration influences iDIS in granulomas. Nonuniform drug distributions within granulomas arise due to barriers to diffusion that the cellular structure of granulomas creates[22–24,32]. The spatial variation in antibiotic concentrations within a granuloma leads to variations in local effective concentrations, and ultimately antibiotic killing rates and iDIS. The free drug concentrations available to induce bactericidal activity against Mtb are also influenced by binding to extracellular matrix as well as partitioning into macrophages[44]. Hence, we next focused on the contribution of the drug spatial variation to iDIS.

Figure 7 shows the spatial variation of both effective drug concentrations and iDIS for each of the four regimens simulated: HRZE, RE, HE and RM. Overall, when antibiotics in a regimen are present in the granuloma

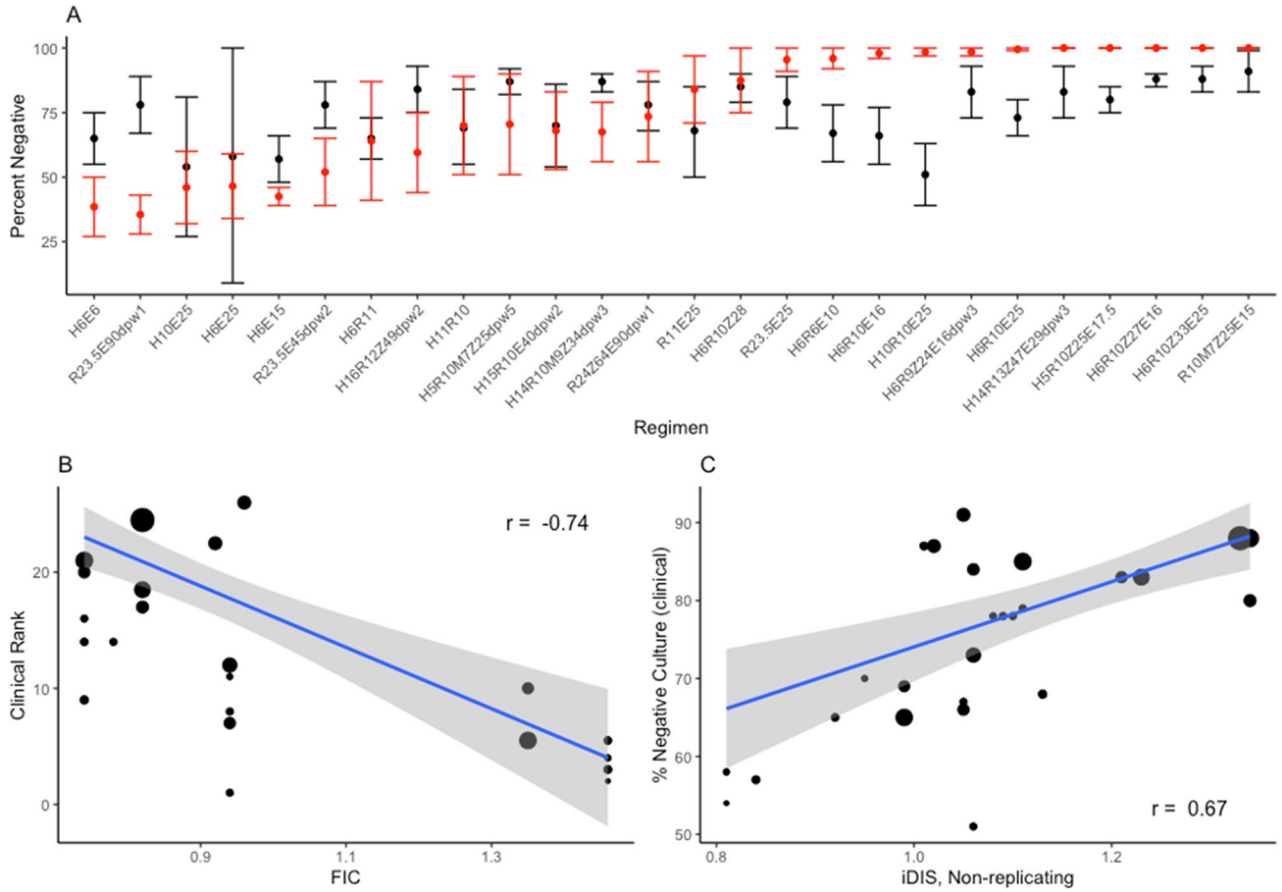

Figure 5. Comparison of treatment simulations with clinical trial results. The results for 26 different regimens compiled in Bonnet et al.[40] are compared to our treatment simulations. The clinical regimen efficacy metric used is solid culture conversion following 8 weeks of therapy. We compare the confidence intervals (black) to the percent of simulated granulomas that sterilized (lower red bar) or had fewer than 10 CFU after 8 weeks of therapy (upper red bar, red dot average of error bars) for all 26 regimens (**A**). Regimens are abbreviated by the single antibiotic abbreviation, followed by the dose in mg/kg for that antibiotic, with the doses per week (dpw) listed at the end of the regimen abbreviation. FIC is negatively correlated with clinical rank with a weighted correlation of −0.74 (**B**), and iDIS is positively correlated with clinical rank with a weighted correlation of 0.67 (**C**). Each dot represents an individual regimen, its size is linearly scaled by the number of patients treated (**B**, **C**). Plots were made using the ggplot2 package in R[39].

at similar relative concentrations, the in vitro interaction is maintained in vivo. Interactions can also be strong in caseated regions of the granuloma, where non-replicating Mtb are typically located. Because iDIS tends to be higher in locations that contain more non-replicating Mtb, this may contribute to synergistic combinations performing better than antagonistic combinations.

An additional aspect that influences the iDIS is the relative contribution of each antibiotic in the combinations (Fig. 7, column 1). Antibiotic combinations that contribute more equally to the effective concentration deviate more from additivity than combinations of antibiotic concentrations in which contributions are uneven (i.e. when one antibiotic has a much higher adjusted concentration than the other antibiotics). Although RE has a more synergistic FIC than HRZE, the iDIS against non-replicating Mtb for HRZE is higher than RE, and HRZE has better efficacy than RE. This is partially due to R and Z contributing to the effective concentration in the granuloma evenly (R ~ 50% contribution, Z ~ 40% contribution). The contributions from R and E in RE, however, are more disproportionate, with > 90% of the effective concentration due to R and < 10% of the effective concentration from E.

A similar situation occurs with the two antagonistic combinations HE and RM. Although RM is predicted to be strongly antagonistic, its efficacy is still average compared across all regimens tested. HE, on the other hand, has a less antagonistic FIC, but performs more poorly than RM. When looking at both antibiotic contributions for these two regimens and the iDIS against non-replicating Mtb, we see that H accounts for ~ 75% of the effective concentration and E accounts for ~ 25%. Although not equal contributions, this still allows for an antagonistic interaction to occur. With the RM combination, R accounts for almost all of the contribution to the effective concentration because its levels are higher relative to its own C_{50}, resulting in almost no antagonistic interaction to occur with M, despite the high FIC. For antagonistic combinations, uneven contributions from the different antibiotics in the combination can mitigate the effect of the antagonistic interaction.

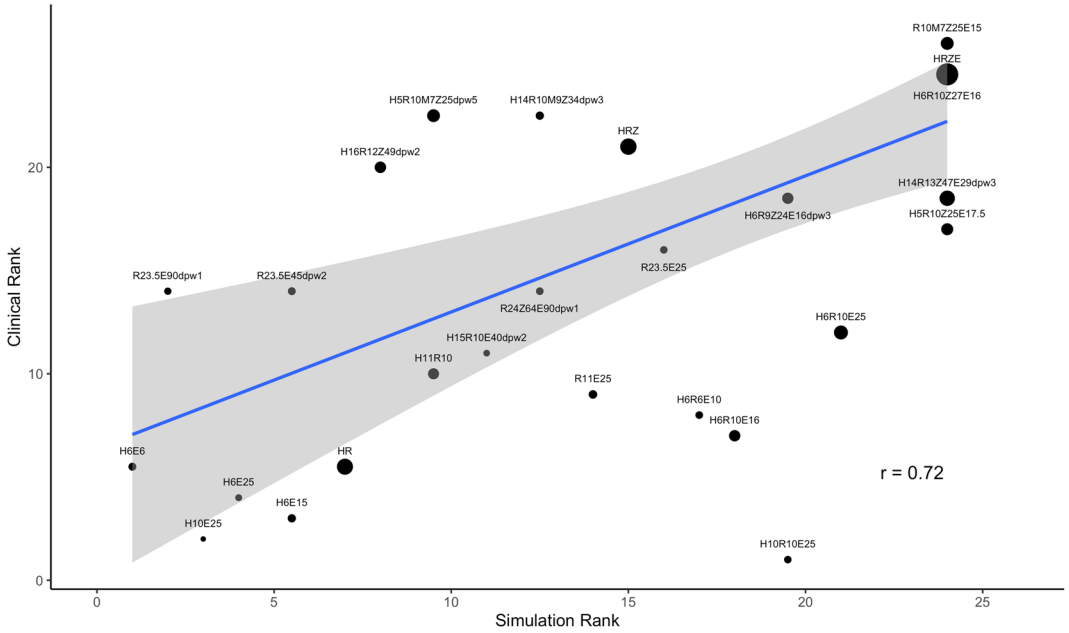

Figure 6. INDIGO-MTB-*GranSim* compared with clinical data. Comparison and validation of treatment simulations with clinical trial results for 26 different regimens compiled in Bonnet et al.[40]. Predictions from *GranSim* simulations for 26 drug regimens correlate with clinical outcomes. The simulation rank, ranked by percentage of sterilized granulomas after 8 weeks, and clinical rank, ranked by clinically reported culture conversion, have a weighted correlation of 0.72, weighted by the number of patients treated with each regimen. Plots were made using the ggplot2 package in R[39].

Due to this dependence on drug concentrations, the predicted iDIS varies for different doses and regimens of the same drug combination (Supplementary Fig. 3). In contrast, the FIC interaction score is fixed for a combination irrespective of the dosage. As doses vary in vivo, the strength of the synergistic or antagonistic interactions can either increase or decrease, depending on the specific combination of antibiotics. One common trend is less frequent dosing tends to decrease the interaction strength, which we observe for both the HRZE and RE combinations.

Plasma clearance rates correlate with in vivo drug interaction score. Even for a given simulated granuloma and drug regimen, antibiotic concentrations can vary due to host-to-host PK variability[34]. This can also result in changes in iDIS. We picked four different regimens, ranging from synergistic to antagonistic (HRZE, RE, HE, RM) to exhaustively explore the impact of various PK parameters. The plasma clearance rate constant for many of the antibiotics in these regimens is significantly correlated with predicted iDIS, particularly the clearance rate constants for R, E and M (Table 1). A more detailed analysis of correlations between plasma PK parameters and iDIS is shown in Supplementary Table 3. The R clearance rate constant is strongly correlated with iDIS, with coefficients between 0.8 and 0.9, depending on the regimen. The correlation coefficients for the clearance rate constant for R are positive for synergistic combinations (HRZE, RE), and negative for antagonistic combinations (RM). Because iDIS values that deviate further from 1 imply a stronger interaction, this means that faster clearance rates for R tend to increase the interaction strength. The opposite is true for the clearance rate constant of E. The correlation coefficient between the clearance rate constant for E and predicted iDIS is negative in synergistic combinations (HRZE, RE), and positive in the antagonistic combination (HE). While this may seem counterintuitive, it supports the idea that the iDIS value is dependent on relative in vivo drug concentrations. Faster clearance rates generally result in lower concentrations in plasma, and consequently lower concentrations in the granuloma. Because R tends to contribute more to effective concentrations than other antibiotics, increasing the clearance rates for R will strengthen the interaction by decreasing R concentration and allow for more similar antibiotic contributions. For E, whose contribution to effective concentration tends to be lower, increasing clearance rates result in lower E concentrations and contributions, and scenarios of even more lopsided contributions and less interaction. Relative drug concentrations inside the granuloma affect the strength of drug interactions, and these strong correlations indicate that interactions may be stronger or weaker for certain combinations depending on an individual's PK[34].

We see a similar trend to plasma PK when analyzing the impact that lung tissue PK parameters have on iDIS. Sensitivity analysis on the tissue PK parameters for different regimens shows that some have a positive correlation and some have a negative correlation with iDIS. Tissue PK parameters that lead to more similar concentrations and contributions of antibiotics results in stronger interactions (Supplementary Table 4). As an example, for the RE regimen, vascular permeability for R is negatively correlated with iDIS of the regimen while vascular permeability for E is positively correlated.

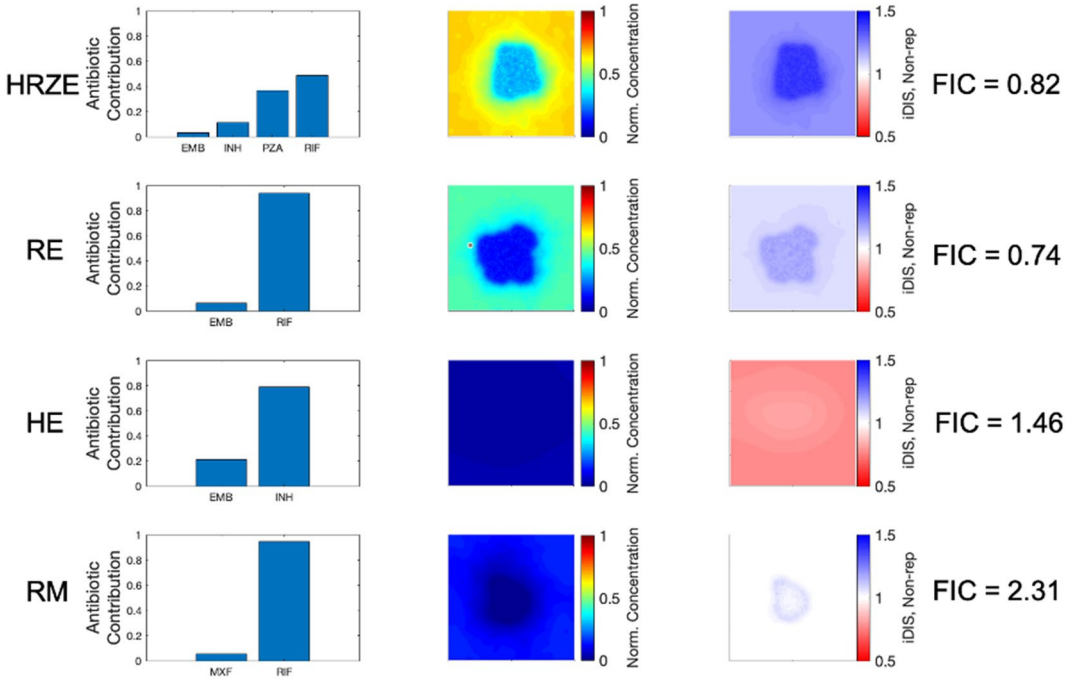

Figure 7. Contribution of individual antibiotics to the in vivo drug interaction score (iDIS). Values of iDIS are associated with the proportion of each antibiotic's contribution to effective concentration. Four different regimens are shown: HRZE (first row), RE (second row), HE (third row), and RM (fourth row). Bar plots indicate the relative contribution of each antibiotic in the regimen to the effective concentration on average throughout the granuloma. Heat maps for each drug combination show the effective concentration normalized to the C_{50} for non-replicating Mtb (second column). The calculated iDIS value for non-replicating Mtb is shown in the fourth column, with the color bar representing the iDIS value: blue represents synergy, white represents additivity, and red represents antagonism. All heat maps reflect conditions 6 h after dosage with each antibiotic in the corresponding regimen. Heat maps and plots were made using MATLAB (R2019a)[45].

Regimen	PRCC values for predicted iDIS		
	R clearance	E clearance	M clearance
HRZE	0.89	−0.56	N/A
RE	0.90	−0.92	N/A
HE	N/A	0.88	N/A
RM	−0.83	N/A	0.99

Table 1. Significant antibiotic clearance rate constants in determining iDIS. The relationship between clearance rate constants for different antibiotics is correlated with iDIS with non-replicating Mtb during the first dose of therapy. Table shows PRCC values relating the clearance rate constants to the predicted iDIS for the regimens HRZE, RE, HE and RM. The values shown represent PRCC values that are significant with $p < 0.01$.

Discussion

There is an urgent need for multi-drug regimens to treat TB, the world's deadliest disease. In particular, understanding the role of synergistic or antagonistic interactions between anti-TB drugs in vivo may provide a more rational approach to choosing novel combinations that have greater clinical efficacy. However, measuring drug interactions in vivo is challenging due to the limited throughput, cost, and time involved in testing drugs in model organisms. In this study, we introduce a computational pipeline that can simulate in vivo interactions by using datasets derived from individual drug-response transcriptomes and PK/PD, thereby greatly reducing cost and time. Our approach integrates interaction scores of combinations of antibiotics into a computational model that simulates drug delivery into the lung, spatial concentrations of drugs and pharmacodynamic effects within TB granulomas.

To evaluate drug regimens, we introduce a new metric called the in vivo drug interaction score (iDIS) that is dynamic and unique for each mycobacterium based on its location and metabolic state (i.e. replicating/non-replicating) within a granuloma. Unlike the in vitro drug interaction scores derived from checkerboard assays

and INDIGO-MTB, which are fixed for given drug combinations, the in vivo score can provide a more nuanced impact of drug interactions on pathogen clearance. This allowed us to compare various drug regimens and rank them based on their in vivo interactions. We found that our ranking of regimens is highly concordant with clinically observed efficacy of various drug combinations[40]. In Fig. 5, we compare the percentage of simulated granulomas that were sterilized after 8 weeks of treatment for 26 different antibiotic regimens, and compared those results to 8-week sputum culture conversion from clinical trials of those same regimens. For regimens where our predicted sterilization does not agree with clinical results, we tend to overpredict sterilization. This could partially be explained by the fact that while we compare sterilization at the granuloma scale, culture conversion reflects a host-level outcome that involves treating and sterilizing multiple granulomas and lesions. Additionally, accounting for different drug–drug interactions depending on a heterogeneous granuloma environment (such as in the caseum) could further improve our ability to accurately predict clinical results[46].

When simulating all regimens considered in this study, the FIC alone does correlate with the simulated and predicted outcomes from our model. However, there are a handful of regimens that do not fit the trend. Measuring the iDIS, which evaluates the relative increase or decrease in killing rate due to the interaction within the complex granuloma environment, provides a complementary measure of regimen outcome. This is because the effect that drug interactions have on killing rate constants is dependent on the balance of contributions from each single antibiotic. Combinations with highly synergistic or antagonistic FIC values may be closer to additive if only one antibiotic is present in sufficient quantities within a granuloma.

Our analysis of various drug regimens revealed ways of amplifying synergy as well mechanisms to mitigate antagonism in vivo. We found that some combinations with in vitro antagonism perform well clinically due to the distinct spatial distribution of the underlying drugs. Antagonistic interactions can be mitigated if the drugs have uneven distributions and effective concentrations or through less frequent dosing. Overall, we find that combinations with strong in vitro synergy remain synergistic or additive in vivo. Hence screening for synergy in vitro can be a useful strategy for identifying regimens with strong in vivo activity. In a minority of cases, this synergy may not be achieved in vivo; nevertheless, synergistic combinations generally outperform antagonistic regimens.

HRZE stands out among the regimens we tested because it has a synergistic interaction (FIC) which is maintained in vivo (iDIS) due to the similar penetration and distribution of the four drugs in the regimen. In contrast, regimens such as RE and RM have dissimilar drug distributions and their in vitro interactions are not observed in vivo. The RE regimen has a synergistic FIC but the dissimilar drug distributions lead to a reduced iDIS. Similarly, RM has a strongly antagonistic FIC but the dissimilar drug distributions lead to reduced antagonism in vivo.

The clinical relationship between plasma PK and regimen efficacy is well established, and can impact the treatment outcomes and the development of resistance[38,47,48]. Measuring PK parameters in patients can help to predict sterilization rates[49]. While the impact of PK on individual drugs can be straightforward to interpret, the relationship between measured PK and efficacy can be complex for multidrug regimens. Our study suggests that changes in interactions likely occur in vivo due to PK variability. Studies that involve measuring variability in PK and the effect on drug interactions could be the subject of future research.

As part of this study, we wanted to determine which combinations of antibiotics are predicted to have strong synergy and antagonism, as well as which combinations are predicted to have high efficacy. We screened 64 combinations and regimens of front-line regimens (HRZE) along with M and L. The clinically used HRZE regimen does outperform other screened combinations, which highlights the need for new drugs to achieve the aim of improving TB treatment. Based on the INDIGO-MTB model, we previously identified drug combinations involving new TB drugs such as bedaquiline that have better synergy than HRZE. Given the concordance between INDIGO-MTB FIC and various clinical metrics observed in this study, the synergistic combinations identified by INDIGO-MTB may be promising leads for further optimization using *GranSim* for reducing treatment time[18].

A limitation to our computational model is that the same FIC value is applied to all Mtb within a simulation, regardless of its environment or metabolic state. It is likely that the strength of a given interaction, or even whether it is synergistic or antagonistic, is dependent on the bacterium's microenvironment in the granuloma[46,50]. Additionally, these simulations represent treatment of primary granulomas in TB disease, and do not necessarily reflect the true and enormous complexity of granuloma lesions that occur during TB disease. Further, as the simulations are at the granuloma scale, relating the outcomes measured by the simulation to clinical outcomes is difficult. The final limitation is that we only considered combinations of six different antibiotics. There are many other antibiotics in use or in development for use to treat TB. Expanding our ability to accurately simulate the PK/PD of additional antibiotics will greatly increase our ability to answer how important drug interactions are in determining regimen efficacy.

In summary, our study addresses an important gap in current methods for identifying promising drug combinations for TB treatment by presenting a new pipeline for evaluating interactions between drugs in vivo. This pipeline provides an additional metric with which to evaluate novel combinations of antibiotics, explain mechanisms of failed regimens, and assist in optimization regimens as we expand our list of potential antibiotics.

Methods

INDIGO-MTB model for predicting drug interactions. INDIGO-MTB identifies interactions between drugs in a combination regimen by utilizing pathogen transcriptomics in response to individual drugs. INDIGO-MTB was built using drug response transcriptome data for 164 drugs, including well known drugs rifampicin, isoniazid, streptomycin, and several fluoroquinolones[8]. The model first generates a drug–gene association network using the transcriptomics data, and the machine-learning algorithm, Random Forest. The algorithm identifies genes that are predictive of drug interaction outcomes using a training data set of known interactions[27]. This trained network model is used to predict interactions for novel drug combinations and provides the Fractional Inhibitory Concentration (FIC) as an output (Fig. 1a). The model can identify all possible 2-way, 3-way,

4-way and 5-way synergistic, additive and antagonistic drug interactions after in silico screening of more than 1 million potential drug combinations. INDIGO-MTB predicted FIC scores to be integrated within *GranSim* were generated for all possible combinations of the first line drugs and two fluoroquinolones (H, R, Z, E, Levofloxacin (L) and Moxifloxacin (M)), as listed in Supplementary Table 1.

GranSim model of granuloma formation and function. *GranSim* is a well-established agent-based model of granuloma formation and function[24,28–31]. It simulates the spatial heterogeneity and bacterial burden of primary TB lesions by simulating the immune response to infection with Mtb in a computational grid representing a small section of lung tissue, with formation of a granuloma as an emergent behavior (Fig. 1b,c). The simulation begins with a single infected macrophage at the center of the grid, and macrophages and T cells are recruited to the site of infection and interact with each other according to immunology-based rules that describe cell movement, activation, cytokine secretion, and killing of bacteria (for a full list of rules see referenced webpage[51]). Bacteria are tracked individually and modeled as individual agents in the simulation, existing in three distinct subpopulations: intracellular (inside macrophages), extracellular replicating and extracellular non-replicating. The effective growth rates of extracellular bacteria are modulated by the number of bacteria in a given grid compartment. The growth rate becomes zero when the carrying capacity for that compartment is reached to reflect the relative availability of nutrients and physical space limitations[30]. Growth rates of extracellular Mtb are also slowed by the presence of caseum (dead cell debris), as a way to estimate the effect of lack of oxygen[52]. The parameter values describing rules and interactions are based on previous *GranSim* studies and evidence from experimental literature and datasets on non-human primates[24,34,53].

Simulation of antibiotic delivery and concentrations within granuloma. We simulate antibiotic delivery within the *GranSim* computational framework as previously described[24,32,34]. Briefly, a plasma PK model simulates absorption into plasma following an oral dose, exchange with peripheral tissue, and first-order elimination from plasma. Flux of antibiotics into the simulation grid is based on the local gradient between the average drug concentration surrounding vascular sources on the agent-based grid and the plasma concentration. Here we use a 200×200 grid representing a 4 mm × 4 mm lung section. The flux is calculated over time as plasma concentrations change within and around each vascular source and allows for delivery or subtraction from the computational lung environment, depending on the direction of the concentration gradient. Once on the grid, antibiotics diffuse, bind to extracellular material (epithelial tissue and caseum), partition within macrophages and degrade (Fig. 1b,c). Based on relative binding and partitioning rates into macrophages, concentrations of intracellular and bound antibiotic are modeled at pseudo-steady state for isoniazid, rifampin, ethambutol and pyrazinamide. The drugs moxifloxacin and levofloxacin exhibit slower rates of binding and partitioning relative to diffusion. Hence the dynamic binding and partitioning of these drugs are modeled using ordinary differential equations[32]. We determined plasma PK parameters by calibration to human data as previously described[22,34,54]. We calibrated tissue PK parameters based on concentrations in rabbit or human lesions[22,32,34,44]. Parameters are listed in Supplementary Tables 5 and 6.

Calculation of antibiotic killing rate and in vivo drug interaction. We calculate the antibiotic killing rate constant using an Emax model (Hill equation) as we have done previously[24], with parameters listed in Supplementary Table 7. This antibiotic killing rate constant is evaluated at each time step for every Mtb in the simulation based on the local grid concentrations as they change over time. The antibiotic killing rate constant (k) is evaluated as

$$k(t) = E_{max}\frac{C_{eff}(t)^h}{C_{eff}(t)^h + {C_{50}}^h} \tag{1}$$

where E_{max} is the maximal killing rate constant, C_{50} is the concentration at which half maximal killing is achieved, h is the Hill coefficient, and C_{eff} is the effective concentration of the antibiotic (or combination of antibiotics). To reflect each antibiotic's unique levels of activity against different sub-populations of bacteria, the PD parameters C_{50}, E_{max} and h vary depending on the location of the bacteria within the granuloma (intracellular, extracellular replicating, or extracellular non-replicating).The relationship between a combination of drug concentrations and pharmacodynamic effect (such as killing and inhibition) is described using the Loewe Additivity model[16,55]. In the Loewe additivity model, a simply additive interaction between two antibiotics is described by

$$\frac{C_1}{IC_{x,1}} + \frac{C_2}{IC_{x,2}} = 1 \tag{2}$$

where $IC_{x,1}$ and $IC_{x,2}$ are the inhibitory concentrations of drugs 1 and 2 that achieve x% inhibition on their own, and C_1 and C_2 are the concentrations that achieve the same level of inhibition in combination. We can convert the concentration of drug 2 to an equipotent concentration of drug 1, shown in Fig. 8 and denoted $C_{2,adj}$. This gives the concentration of drug 1 that results in the same antibiotic killing rate constant as the given concentration of drug 2 (C_2), which we define as the adjusted concentration for drug 2 ($C_{2,adj}$)

$$C_1 = C_{2,adj} = \left(\frac{{C_{1,50}}^{h_1}{C_2}^{h_2}}{\frac{E_{max,1}}{E_{max,2}}\left({C_2}^{h_2} + {C_{50,2}}^{h_2}\right) - {C_2}^{h_2}}\right)^{1/h_1}, \tag{3}$$

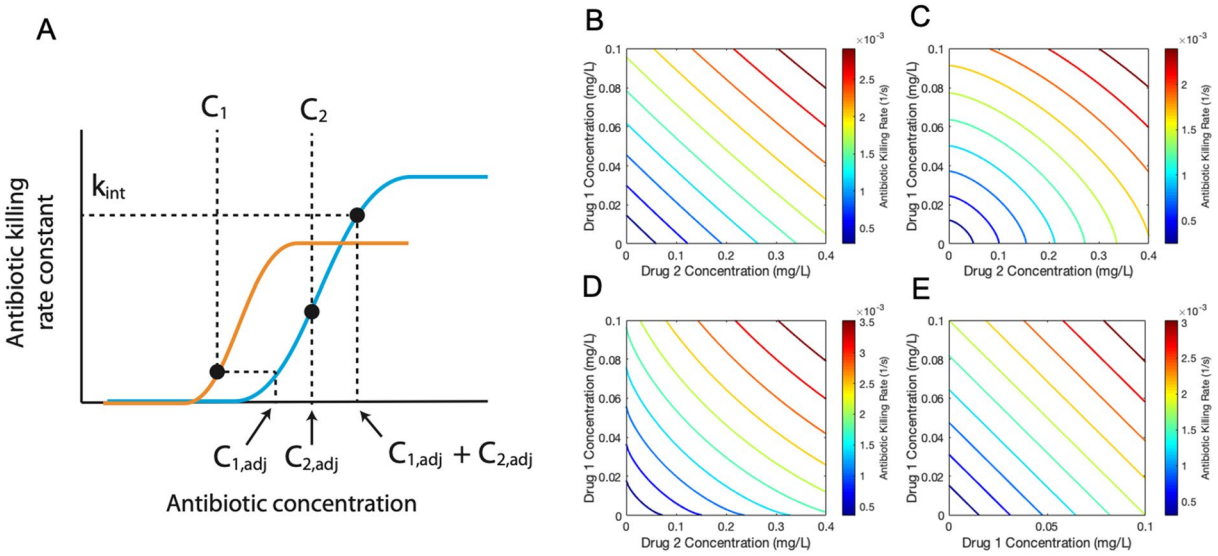

Figure 8. Graphical representation of computing the adjusted concentration and killing rate constant (Eqs. 1 and 3). The adjusted concentration of a drug is found by computing the equipotent concentration for another drug. The plot of two Hill curves for three different drugs (drug 1, orange; drug 2, blue) shows the relationship between concentrations of the two antibiotics and their adjusted concentration (**A**). The effective concentration, evaluated as the sum of the adjusted concentrations, determines the antibiotic killing rate constant. Antibiotic killing rate constant contours show the behavior of the drug interaction model for a combination of two theoretical drugs. Drug 1 has a c50 of 1 mg/L, E_{max} of 0.02 1/s, and a Hill coefficient of 1. Drug 2 has a c50 of 2 mg/L, E_{max} of 0.01 1/s, and a Hill coefficient of 1. When the two drugs have an FIC of 1.0 (**B**), 1.5 (**C**), or 0.6 (**D**), the contours show the characteristic straight line or curved contours characteristic of checkerboard assays for additive, antagonistic, or synergistic combinations. A sham combination of Drug 1 (**E**) results in a simply additive case. Contour plots were made using MATLAB (R2019a)[45].

The corresponding inhibitory concentrations for a given x% inhibition for drugs 1 and 2 are now both equivalent to $IC_{x,1}$, because both C_1 and $C_{2,adj}$ are expressed in terms of concentration of drug 1. Substituting $C_{2,adj}$ for C_2 and $IC_{x,2}$ for $IC_{x,1}$, Equation (2) can be rewritten as

$$C_1 + C_{2,adj} = IC_{x,1}. \tag{4}$$

If there are three or more drugs under consideration, we define this sum of concentrations as the effective concentration (C_{eff}) of a combination of n antibiotics:

$$C_{eff} = \sum_{i=1}^{n} C_{i,adj} \tag{5}$$

We define synergy or antagonism between two or more drugs based on deviations from simple additivity, as assumed above. This deviation is represented using the Fractional Inhibitory Concentration (FIC)[56]:

$$FIC = \frac{C_o}{C_e} \tag{6}$$

where C_o represents the observed combined drug concentration to yield a given level of inhibition, and C_e is the expected combined drug concentration to yield the same level of inhibition if the two drugs or more drugs were simply additive[16]. The FIC measures changes in potency, i.e. how much drug is needed to produce a certain pharmacodynamic effect. Based on the value of FIC, synergistic or antagonistic combinations result in a lower or higher effective drug concentration to achieve the same level of killing. To incorporate drug interactions into our model, we assume the effective concentration for a combination of n drugs is adjusted from Eq. (5) based on the FIC value:

$$C_{eff} = \left(\sum_{i=1}^{n} C_{i,adj}{}^{FIC} \right)^{1/FIC} \tag{7}$$

Equation (7) adjusts effective concentration so that synergistic combinations (FIC < 1) result in a higher effective concentration, and antagonistic combinations (FIC > 1) result in a lower effective concentration. Using our defined effective concentration, we substitute Eq. (7) into Eq. (1) to evaluate the antibiotic killing rate constant for combinations of antibiotics while also accounting for drug interactions. Our drug interaction model and effective concentration formulae accurately recreate in vitro drug interaction behavior observed in checkerboard assays (Fig. 8)[16].

To evaluate the impact that each drug interaction has on the calculated killing rate constant (Eq. 1) for a given combination of antibiotics in our in vivo simulation, we define an in vivo *Drug Interaction Score* (iDIS). The iDIS is the ratio of the bacterial killing rate constant with a predicted FIC to the killing rate constant if FIC was equal to 1, i.e. no or additive drug interactions. This allows us to quantify the impact that drug interactions have on bacterial killing for each individual Mtb at each time step during simulated treatment.

Antibiotic treatment simulations and calculation of regimen efficacy. To simulate treatment with different antibiotic combinations, we first created an in silico granuloma library to generate a set of granulomas. Each library consists of 500 granulomas simulations, generated from 100 parameter sets sampled with Latin Hypercube Sampling (LHS), and each parameter set was replicated five times[57,58]. Supplementary Table 2 lists the parameters varied and their ranges, which have been established in previous work[24,34]. Parameter ranges capture natural variability in the immune response and lung environment, such as differences in cellular recruitment and immune cell activation. In addition, replicating simulations with the same parameter set incorporates variability due to stochasticity in the simulations. Granulomas are simulated for 300 days in the absence of antibiotics. At day 300, a random sample of 100 unsterilized granulomas is selected from the relevant library for treatment. The prescribed regimens are simulated for 180 days or until the granuloma is sterilized. See Supplementary Table 1 for the full list of regimens tested.

We evaluate three metrics from our simulations to assess the efficacy of each regimen tested: log decrease in CFU per day, percent of simulated granulomas that are sterilized after 8 weeks of treatment (sterilization percent), and average time at which those granulomas become sterile (sterilization time). For each regimen, 100 granulomas are simulated and results from those simulations are used to calculate three outcomes measures: simulated log decrease in CFU per day, sterilization percent, and sterilization time.

Comparison to clinical trials. To validate our model results, we compared our treatment simulation outcomes to Phase IIb clinical trial data[40]. We compared the clinical datasets outcomes for each regimen with our simulated granuloma sterilizations after 8 weeks of treatment. We used the percent of granulomas that are completely sterilized at 8 weeks as a lower bound estimate. Our upper bound estimate is the percentage of granulomas with fewer than 10 CFU after 8 weeks. We chose this value as these granulomas with low bacterial load would not be detectable in sputum. Additionally, we compared the rank of clinically tested regimens, ranked by sputum conversion, to the rank of regimens based on simulation results. Simulated regimen rankings were ranked by average sterilization time, FIC, and average iDIS for non-replicating Mtb. Further, we compared our predicted treatment sterilization times for fluoroquinolone-containing regimens with clinical endpoints (up to 6 months) from recent phase III clinical trials that include fluoroquinolones for treating drug-susceptible TB[41–43].

Plasma and tissue PK sensitivity analysis on interaction strength. We performed a sensitivity analysis to evaluate how PK parameters impact the predicted iDIS for regimens with different levels of synergy. For four regimens (HRZE, RE, HE, RM), we selected a single granuloma to simulate treatment for 1 day to measure an iDIS. For each regimen, we simulated the granuloma 500 times with different plasma PK parameters sampled using LHS. For each plasma PK parameter set, we calculated the average iDIS over the first day of dosing over all non-replicating Mtb. We repeated this process for sensitivity analysis on tissue PK parameter, simulating the granuloma 500 times with different tissue PK parameters sampled using LHS. Finally, we evaluated the partial ranked correlation coefficient (PRCC) between each PK parameter and the predicted iDIS to determine the impact each parameter has on the drug interactions[58,59].

Received: 3 September 2020; Accepted: 22 February 2021
Published online: 11 March 2021

References

1. Dheda, K., Barry, C. E. & Maartens, G. Tuberculosis. *Lancet* **387**, 1211–1226 (2016).
2. Global tuberculosis report 2019. Geneva: World Health Organization; 2019. License: CC BY-NC-SA 3.0 IGO (2019).
3. Zumla, A. *et al.* Tuberculosis treatment and management-an update on treatment regimens, trials, new drugs, and adjunct therapies. *Lancet Respir. Med.* **3**, 220–234 (2015).
4. Mdluli, K., Kaneko, T. & Upton, A. The tuberculosis drug discovery and development pipeline and emerging drug targets. *Cold Spring Harb. Perspect. Med* **5**, a021154 (2015).
5. Falzon, D. *et al.* World Health Organization treatment guidelines for drug-resistant tuberculosis, 2016 update. *Eur. Respir. J.* **49**, 1602308 (2017).
6. Conradie, F. *et al.* Treatment of highly drug-resistant pulmonary tuberculosis. *N. Engl. J. Med.* **382**, 893–902 (2020).
7. Xu, J. *et al.* Contribution of pretomanid to novel regimens containing bedaquiline with either linezolid or moxifloxacin and pyrazinamide in murine models of tuberculosis. *Antimicrob. Agents Chemother.* **63**, 1–14 (2019).
8. Ma, S. *et al.* Transcriptomic signatures predict regulators of drug synergy and clinical regimen efficacy against tuberculosis. *MBio* **10**, 1–16 (2019).
9. Berenbaum, M. C. A method for testing for synergy with any number of agents. *J. Infect. Dis.* **137**, 122–130 (1978).
10. Berenbaum, M. C. What is synergy?. *Pharmacol. Rev.* **1989**, 93–141 (1989).
11. Zhu, C., Liu, Y., Hu, L., Yang, M. & He, Z. G. Molecular mechanism of the synergistic activity of ethambutol and isoniazid against *Mycobacterium tuberculosis*. *J. Biol. Chem.* **293**, 16741–16750 (2019).
12. Lobritz, M. A. *et al.* Antibiotic efficacy is linked to bacterial cellular respiration. *Proc. Natl. Acad. Sci. USA* **112**, 8173–8180 (2015).
13. Michel, J. B., Yeh, P. J., Chait, R., Moellering, R. C. & Kishony, R. Drug interactions modulate the potential for evolution of resistance. *PNAS* **105**, 14918–14923 (2008).

14. Chandrasekaran, S. *et al.* Chemogenomics and orthology-based design of antibiotic combination therapies. *Mol. Syst. Biol.* **12**, 872 (2016).
15. Silva, A. *et al.* Output-driven feedback system control platform optimizes combinatorial therapy of tuberculosis using a macrophage cell culture model. *PNAS* **113**, 2172–2179 (2016).
16. Cokol, M., Kuru, N., Bicak, E., Larkins-Ford, J. & Aldridge, B. B. Efficient measurement and factorization of high-order drug interactions in *Mycobacterium tuberculosis*. *Sci. Adv.* **3**, e1701881 (2017).
17. Yeh, P., Tschumi, A. I. & Kishony, R. Functional classification of drugs by properties of their pairwise interactions. *Nat. Genet.* **38**, 489–494 (2006).
18. Cicchese, J. M., Pienaar, E., Kirschner, D. E. & Linderman, J. J. Applying optimization algorithms to tuberculosis antibiotic treatment regimens. *Cell. Mol. Bioeng.* **10**, 523–535 (2017).
19. Fonseca, K. L., Rodrigues, P. N. S., Olsson, I. A. S. & Saraiva, M. Experimental study of tuberculosis: From animal models to complex cell systems and organoids. *PLoS Pathog.* **13**, 1–13 (2017).
20. Lin, P. L. *et al.* Quantitative comparison of active and latent tuberculosis in the cynomolgus macaque model. *Infect. Immun.* **77**, 4631–4642 (2009).
21. Dartois, V. The path of anti-tuberculosis drugs: From blood to lesions to mycobacterial cells. *Nat. Rev. Microbiol.* **12**, 159–167 (2014).
22. Prideaux, B. *et al.* The association between sterilizing activity and drug distribution into tuberculosis lesions. *Nat. Med.* **21**, 1223–1227 (2015).
23. Sarathy, J. P. *et al.* Prediction of drug penetration in tuberculosis lesions. *ACS Infect. Dis.* **2**, 552–563 (2016).
24. Pienaar, E. *et al.* A computational tool integrating host immunity with antibiotic dynamics to study tuberculosis treatment. *J. Theor. Biol.* **367**, 166–179 (2015).
25. Sarathy, J. P. *et al.* Extreme drug tolerance of *mycobacterium tuberculosis* in Caseum. *Antimicrob. Agents Chemother.* **62**, 1–11 (2018).
26. Bowness, R., Chaplain, M. A. J., Powathil, G. G. & Gillespie, S. H. Modelling the effects of bacterial cell state and spatial location on tuberculosis treatment: Insights from a hybrid multiscale cellular automaton model. *J. Theor. Biol.* **446**, 87–100 (2018).
27. Chandrasekaran, S. Predicting drug interactions from chemogenomics using INDIGO. *Syst. Chem. Biol. Methods Mol. Biol.* (ed. Ziegler S. and Waldmann H.)**1888**, 219–231 (Humana Press, 2019).
28. Segovia-Juarez, J. L., Ganguli, S. & Kirschner, D. Identifying control mechanisms of granuloma formation during *M. tuberculosis* infection using an agent-based model. *J. Theor. Biol.* **231**, 357–376 (2004).
29. Cilfone, N. A., Perry, C. R., Kirschner, D. E. & Linderman, J. J. Multi-scale modeling predicts a balance of tumor necrosis factor-a and interleukin-10 controls the granuloma environment during Mycobacterium truberculosis infection. *PLoS ONE* **8**, e68680 (2013).
30. Ray, J. C. J., Flynn, J. L. & Kirschner, D. E. Synergy between individual TNF-dependent functions determines granuloma performance for controlling *Mycobacterium tuberculosis* infection. *J. Immunol.* **812**, 3706–37017 (2009).
31. Fallahi-Sichani, M., El-Kebir, M., Marino, S., Kirschner, D. E. & Linderman, J. J. Multiscale computational modeling reveals a critical role for TNF-α receptor 1 dynamics in tuberculosis granuloma formation. *J. Immunol.* **186**, 3472–3483 (2011).
32. Pienaar, E. *et al.* Comparing efficacies of moxifloxacin, levofloxacin and gatifloxacin in tuberculosis granulomas using a multi-scale systems pharmacology approach. *PLOS Comput. Biol.* **13**, e1005650 (2017).
33. Pienaar, E., Dartois, V., Linderman, J. J. & Kirschner, D. E. In silico evaluation and exploration of antibiotic tuberculosis treatment regimens. *BMC Syst. Biol.* **9**, 1–12 (2015).
34. Cicchese, J. M., Dartois, V., Kirschner, D. E. & Linderman, J. J. Both pharmacokinetic variability and granuloma heterogeneity impact the ability of the first-line antibiotics to sterilize tuberculosis granulomas. *Front. Pharmacol.* **11**, 1–15 (2020).
35. Pienaar, E., Linderman, J. J. & Kirschner, D. E. Emergence and selection of isoniazid and rifampin resistance in tuberculosis granulomas. *PLoS ONE* **13**, 1–29 (2018).
36. Strydom, N. *et al.* Tuberculosis drugs' distribution and emergence of resistance in patient's lung lesions: A mechanistic model and tool for regimen and dose optimization. *PLoS Med.* **16**, e1002773 (2019).
37. Aljayyoussi, G. *et al.* Pharmacokinetic-Pharmacodynamic modelling of intracellular *Mycobacterium tuberculosis* growth and kill rates is predictive of clinical treatment duration. *Sci. Rep.* **7**, 1–11 (2017).
38. Pasipanodya, J. G. *et al.* Serum drug concentrations predictive of pulmonary tuberculosis outcomes. *J. Infect. Dis.* **208**, 1464–1473 (2013).
39. Wickham, H. *ggplot2: Elegant Graphics for Data Analysis* (Springer-Verlag, 2016).
40. Bonnett, L. J., Ken-dror, G., Koh, G. C. K. W. & Davies, G. R. Comparing the efficacy of drug regimens for pulmonary tuberculosis: Meta-analysis of endpoints in early-phase clinical trials. *Clin. Infect. Dis.* **65**, 46–54 (2017).
41. Gillespie, S. H. *et al.* Four-month moxifloxacin-based regimens for drug-sensitive tuberculosis. *N. Engl. J. Med.* **371**, 1577–1587 (2014).
42. Jindani, A. *et al.* High-dose rifapentine with moxifloxacin for pulmonary tuberculosis. *N. Engl. J. Med.* **371**, 1599–1608 (2014).
43. Pranger, A. D., van der Werf, T. S., Kosterink, J. G. W. & Alffenaar, J. W. C. The role of fluoroquinolones in the treatment of tuberculosis in 2019. *Drugs* **79**, 161–171 (2019).
44. Zimmerman, M. *et al.* Ethambutol partitioning in tuberculous pulmonary lesions explains its clinical efficacy. *Antimicrob. Agents Chemother.* **61**, 1–12 (2017).
45. MATLAB. *version 9.6.0.1072779 (R2019a)*. (The MathWorks Inc., 2019).
46. Cokol, M., Li, C. & Chandrasekaran, S. Chemogenomic model identifies synergistic drug combinations robust to the pathogen microenvironment. *PLoS Comput. Biol.* **14**, 1–24 (2018).
47. Pasipanodya, J. G., Srivastava, S. & Gumbo, T. Meta-analysis of clinical studies supports the pharmacokinetic variability hypothesis for acquired drug resistance and failure of antituberculosis therapy. *Clin. Infect. Dis.* **55**, 169–177 (2012).
48. Swaminathan, S. *et al.* Drug concentration thresholds predictive of therapy failure and death in children with tuberculosis: Bread crumb trails in random forests. *Clin. Infect. Dis.* **63**, S63–S74 (2016).
49. Chigutsa, E. *et al.* Impact of nonlinear interactions of pharmacokinetics and mics on sputum bacillary kill rates as a marker of sterilizing effect in tuberculosis. *Antimicrob. Agents Chemother.* **59**, 38–45 (2015).
50. Zimmermann, M. *et al.* Integration of metabolomics and transcriptomics reveals a complex diet of *Mycobacterium tuberculosis* during. *mSystems* **2**, 1–18 (2017).
51. GranSim. http://malthus.micro.med.umich.edu/GranSim/. (Accessed 21 August 2020)
52. Pienaar, E., Matern, W. M., Linderman, J. J., Bader, J. S. & Kirschner, D. E. Multiscale model of *Mycobacterium tuberculosis* infection maps metabolite and gene perturbations to granuloma sterilization. *Infect. Immun.* **84**, 1650–1669 (2016).
53. Cilfone, N. A. *et al.* Computational modeling predicts IL-10 control of lesion sterilization by balancing early host immunity-mediated antimicrobial responses with caseation during *Mycobacterium tuberculosis* infection. *J. Immunol.* **194**, 664–677 (2015).
54. Jonsson, S. *et al.* Population pharmacokinetics of ethambutol in South African tuberculosis patients. *Antimicrob. Agents Chemother.* **55**, 4230–4237 (2011).
55. Greco, W. R., Bravo, G. & Parsons, J. C. The search for synergy: A critical review from a response surface perspective. *Pharmacol. Rev.* **47**, 331–385 (1995).

56. Hall, M. J., Middleton, R. F. & Westmacott, D. The fractional inhibitory concentration (FIC) index as a measure of synergy. *J. Antimicrob. Chemother.* **11**, 427–433 (1983).
57. McKay, A. M. D., Beckman, R. J. & Conover, W. J. A comparison of three methods for selecting values of input variables in the analysis of output from a computer code. *Technometrics* **21**, 239–245 (1979).
58. Marino, S., Hogue, I. B., Ray, C. J. & Kirschner, D. E. A methodology for performing global uncertainty and sensitivity analysis in systems biology. *J. Theor. Biol.* **254**, 178–196 (2008).
59. Renardy, M., Hult, C., Evans, S., Linderman, J. J. & Kirschner, D. E. Global sensitivity analysis of biological multiscale models. *Curr. Opin. Biomed. Eng.* **11**, 109–116 (2019).

Acknowledgements

This research was supported by the following grants from the National Institutes of Health: U01HL131072 (to DK, JL) and R01AI123093 and R01AI150684 (awarded to DK) and UL1TR002240, U19AI106761 (to SC), We also acknowledge funds from University of Michigan (UM) Precision Health (SC, DK, JL), UM Office of the Vice Provost of Research (SC) and UM MCUBED (SC, DK). Simulations used resources of the National Energy Research Scientific Computing Center, which is supported by the Office of Science of the U.S. Department of Energy under Contract No. ACI-1053575 and the Extreme Science and Engineering Discovery Environment (XSEDE), which is supported by National Science Foundation grant MCB140228. We thank Paul Wolberg for computational assistance and support.

Author contributions

The simulations presented in this work were completed by J.C. S.C. and A.S. provided FIC predictions from INDIGO-MTB. J.C., D.K., and J.L. provided the simulation framework *GranSim*. All authors (J.C., A.S., D.K., J.L., S.C.) contributed to the conceptualization of this work, analysis of results, and writing and editing.

Competing interests

The authors declare no competing interests.

Additional information

Supplementary Information The online version contains supplementary material available at https://doi.org/10.1038/s41598-021-84827-0.

Correspondence and requests for materials should be addressed to D.K., J.L. or S.C.

Reprints and permissions information is available at www.nature.com/reprints.

Publisher's note Springer Nature remains neutral with regard to jurisdictional claims in published maps and institutional affiliations.